

Figure S1 (a) The *C. elegans* SWI/SNF complex. Two putative subclasses, analogous to mammalian BAF and PBAF, are distinguished by their association with exclusive signature subunits. Subunits investigated during this study are coloured, with the catalytic subunit depicted in red and signature subunits depicted in orange or purple. (b) List of the various predicted *C. elegans* SWI/SNF subunits and their orthologs in yeast, fly and human. Adapted from^{11,12,15}. (c) Expression/Localization

of DAF-16/FOXO and SWI/SNF. *C. elegans* of the indicated genotypes were grown asynchronously. *e1370ts* was inactivated by a shift for 20 h to restrictive temperature. GFP signal in L3 larvae is shown. Yellow lines indicate positions of the cuticle and pharynx. Red arrows indicate sample neuronal nuclei. Green arrowheads indicate sample intestinal nuclei. (scale bar: 20 μ m) (The anatomical sketch was adapted from wormbase.org.)

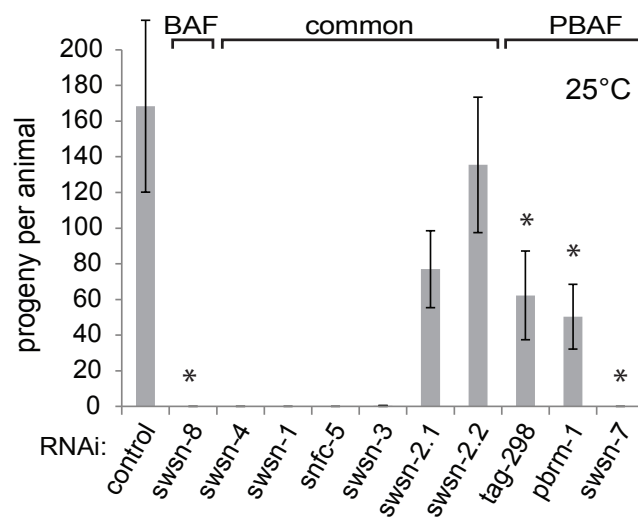


Figure S2 Validation of RNAi conditions for the various SWI/SNF signature subunits. Mostly independent from its involvement with DAF-16/FOXO, loss of either the BAF or PBAF SWI/SNF subclasses leads to defects in germline development¹⁵, which results in reduced brood-size. We used this phenotype to validate the efficiency of our SWI/SNF subunit RNAi conditions. In parallel to the experiments from Figure 2b,d, wild-type *C. elegans* were

seeded as L1 onto the indicated RNAi bacteria and grown at 25°C. Progeny for individual animals between days 1 and 3 of adulthood was counted (n=22 animals; error bars based on S.D. between animals). RNAi for all the BAF and PBAF signature subunits yielded significantly reduced brood sizes compared to control conditions (*; t-Test; p<0.05), suggesting that those RNAi conditions worked reasonably well.

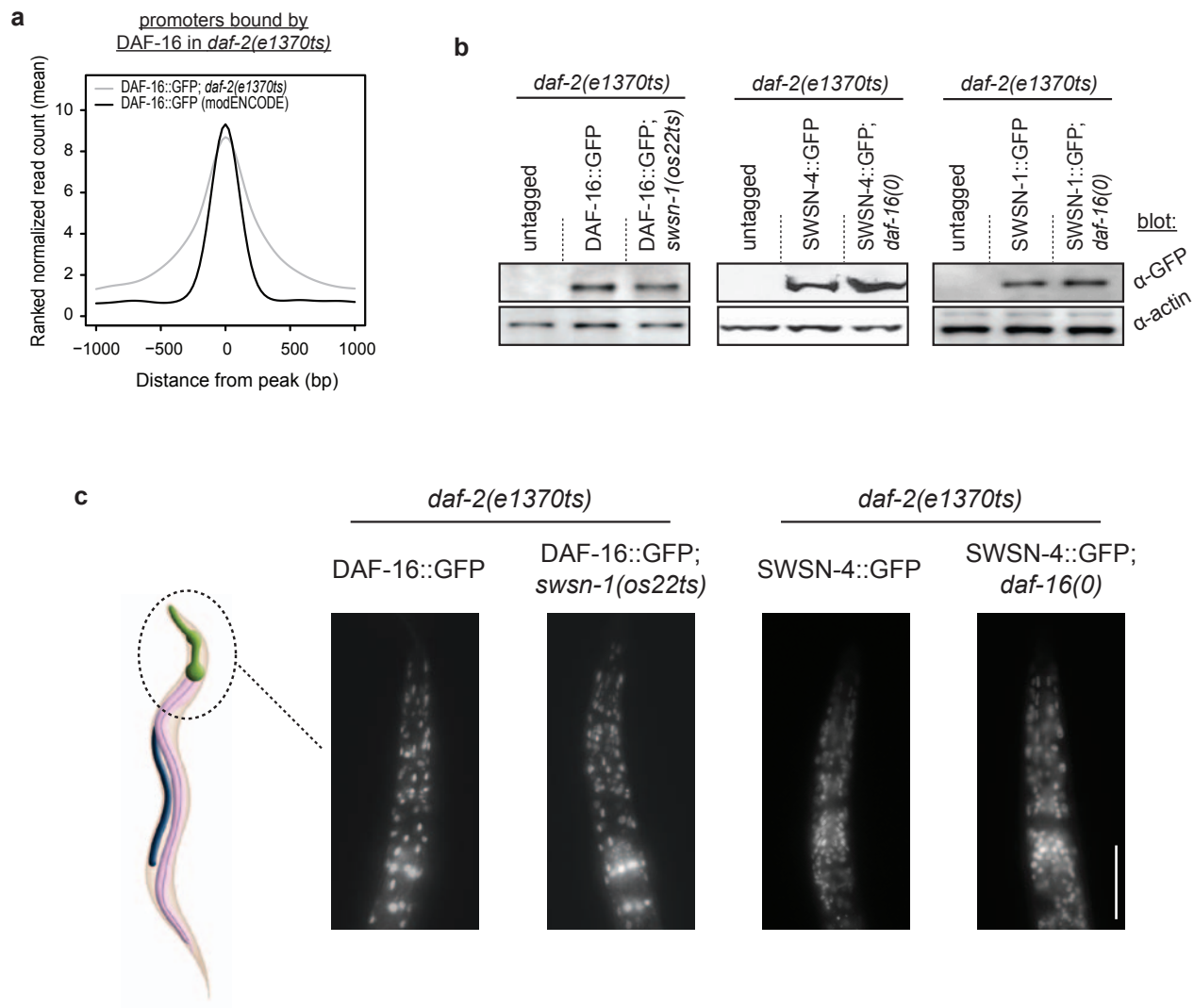


Figure S3 (a) Good correlation of our DAF-16/FOXO ChIP-Seq dataset from *daf-2(e1370ts)* with a previous dataset from wild-type animals. Our ChIP-Seq data for DAF-16/FOXO::GFP; *daf-2(e1370ts)* from Figure 4 was compared to data for DAF-16/FOXO::GFP from wild-type animals, previously made available by the modENCODE consortium⁴. Mean read distributions from the two datasets across our DAF-16/FOXO binding sites are shown. (b,c) DAF-16/FOXO and SWI/SNF do not affect each other's expression levels

or nuclear localization. *C. elegans* were grown asynchronously; *e1370ts* and *os22ts* alleles were inactivated by a 20h shift to restrictive temperature. (b) Whole worm lysates of indicated strains were analysed by SDS-PAGE and western blotting. (c) GFP signal in L4/YA animals of indicated strains is shown. SWSN-1::GFP showed results identical to SWSN-4::GFP (data not shown). (scale bar: 100 μm) (The anatomical sketch was adapted from wormbase.org.)

α -GFP-ChIP:

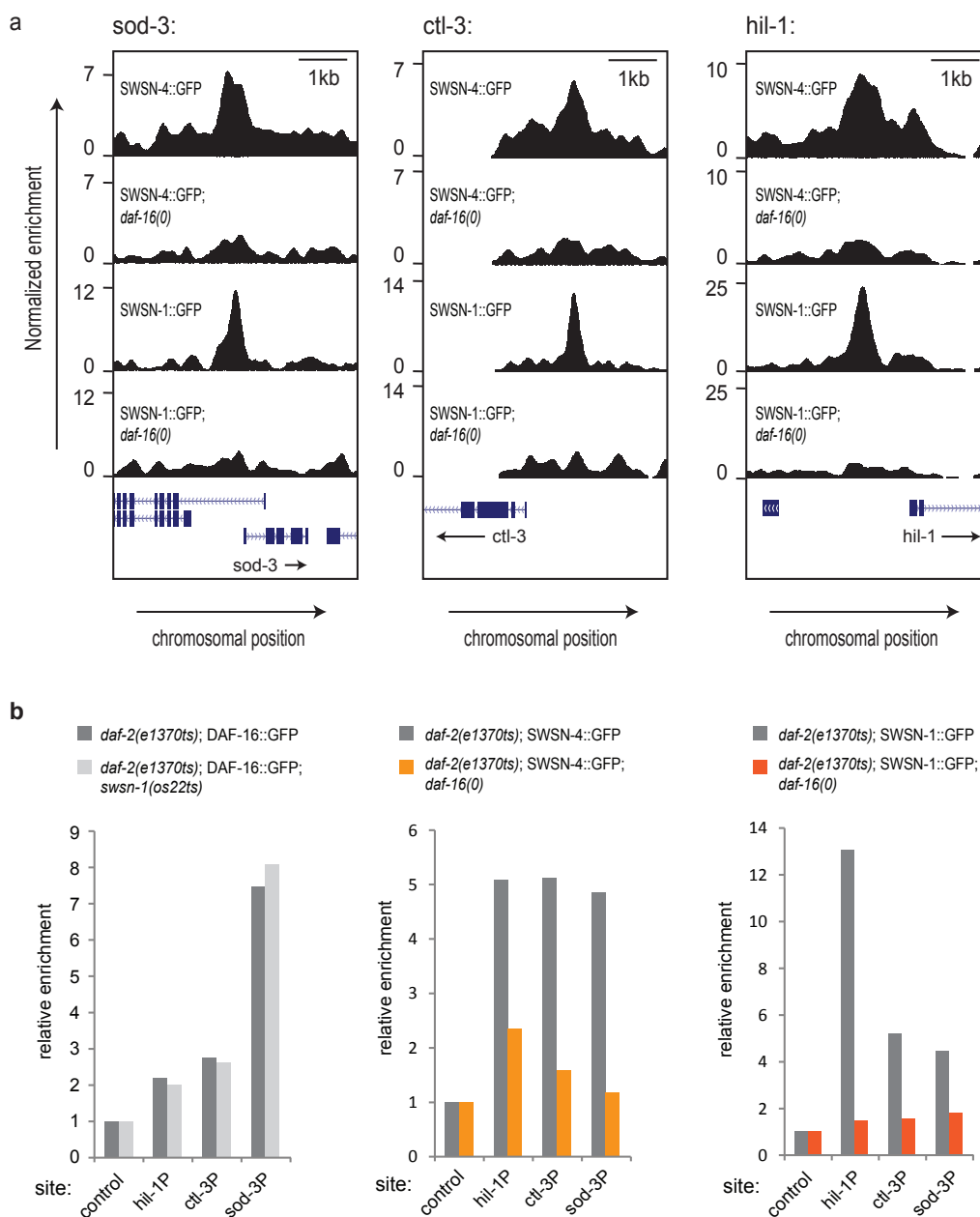
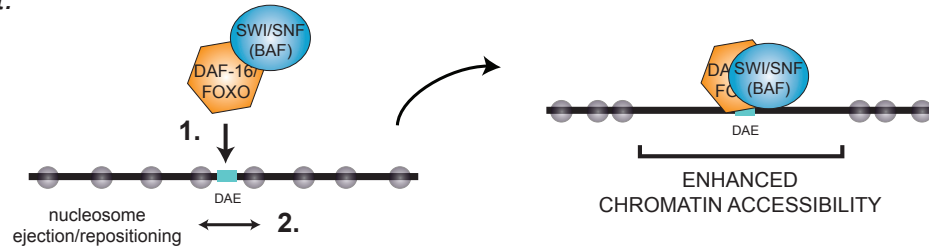


Figure S4 (a) *daf-16(0)*-dependent changes in SWI/SNF binding at prominent promoter regions that are directly bound and activated by DAF-16/FOXO. SWSN-4::GFP and SWSN-1::GFP ChIP-Seq data from Figures 5b and 5c was normalized, smoothed over 50 bp bins,

and displayed in the UCSC genome browser. *sod-3*, *ctl-3*, and *hil-1* promoter regions are shown. (b) Confirmation of the ChIP-Seq data for *sod-3*, *ctl-3*, and *hil-1* promoter regions by conventional ChIP-qPCR.

a

General concept:



Gene activation by DAF-16/FOXO-SWI/SNF:

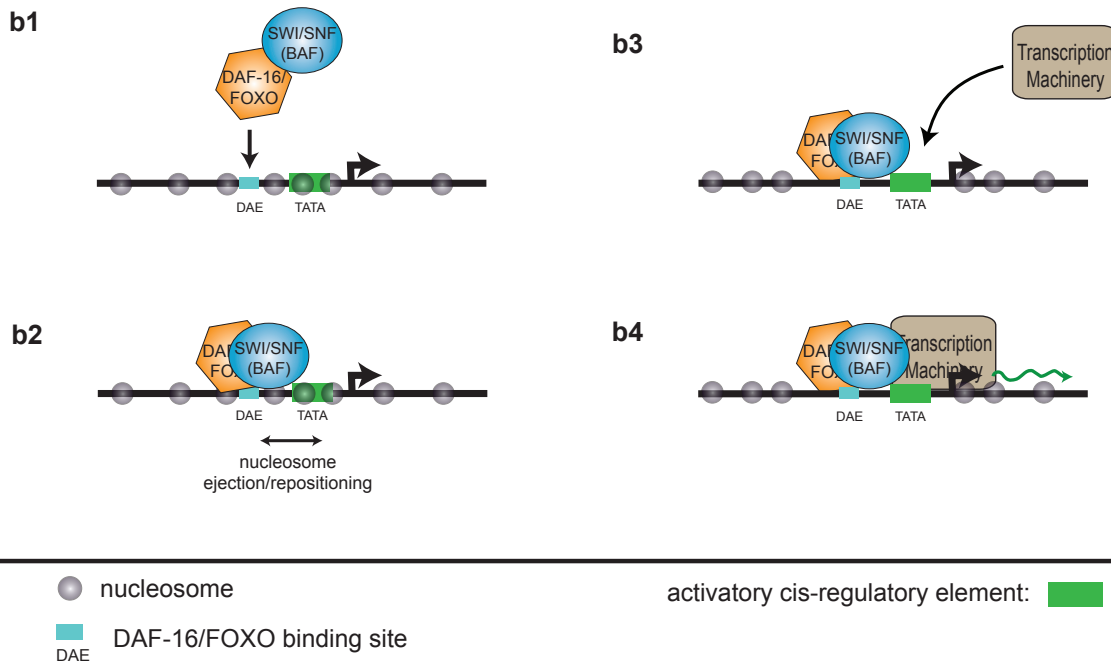


Figure S5 Model for target gene activation by DAF-16/FOXO and SWI/SNF. **(a)** General concept of SWI/SNF recruitment creating a zone of low nucleosome occupancy. This zone allows for better accessibility of contained cis-regulatory elements for binding by downstream components. **(b)** Activation of a target gene by DAF-16/FOXO-SWI/SNF, using the example of a DAF-16/FOXO binding site in proximity to an activatory cis-regulatory

promoter element, the TATA box. **(b1)** DAF-16/FOXO binds to its binding site and recruits SWI/SNF(BAF) to this location. **(b2)** Chromatin remodelling by SWI/SNF(BAF) creates a zone of low nucleosome occupancy. **(b3)** The TATA-box is now accessible for binding by the transcription machinery. **(b4)** Transcription is induced. This model is consistent with previously described roles of SWI/SNF as a transcriptional regulatory cofactor²².

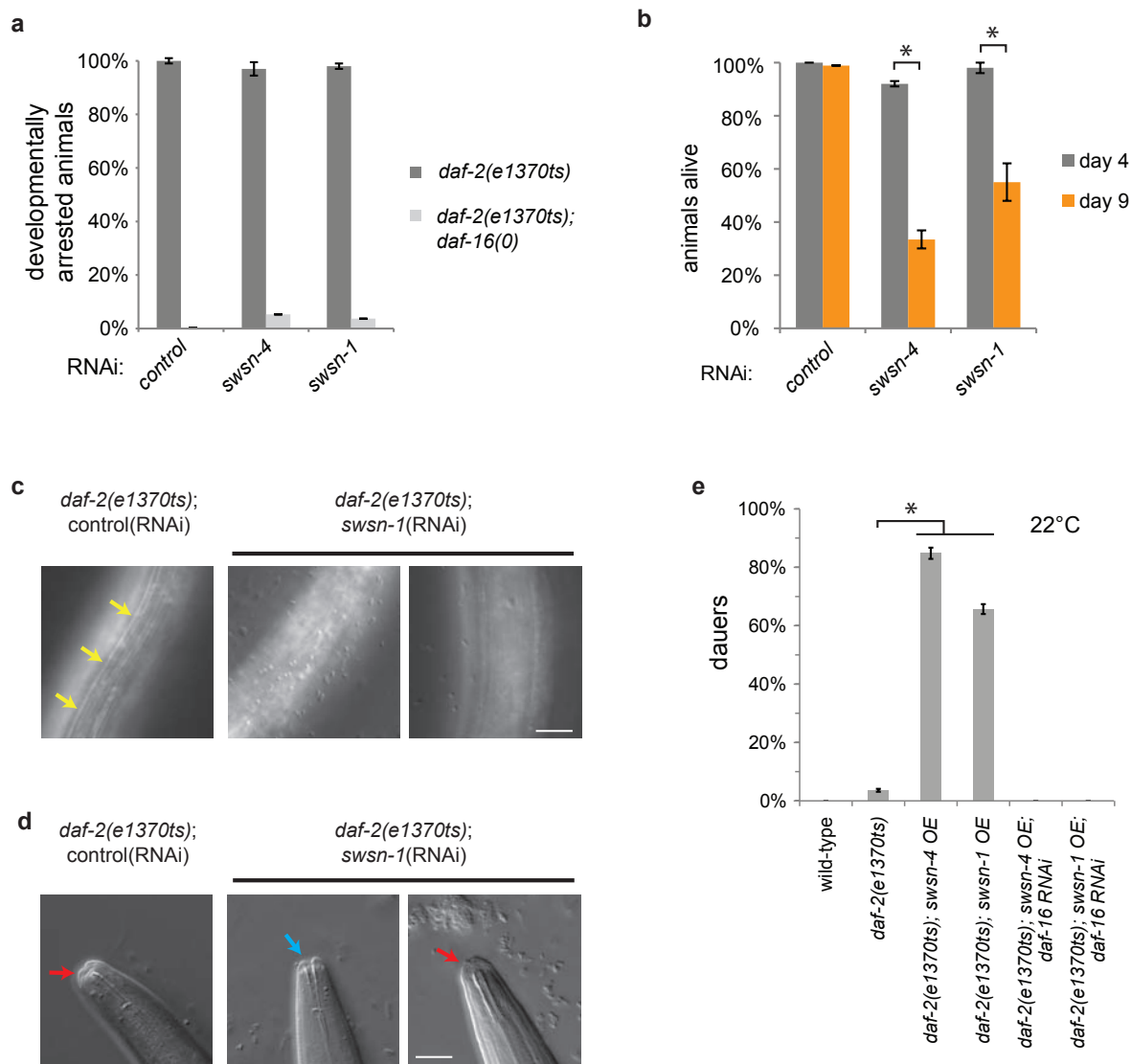


Figure S6 Regulation of dauer formation by SWI/SNF. In *daf-2* mutants, absence of SWI/SNF still allows for DAF-16/FOXO-dependent developmental arrest around the L3 stage (a), but those arrested worms lack typical dauer features (b-d). (a) In parallel to the experiments from Fig. 6a, indicated *C. elegans* strains were seeded onto the indicated RNAi bacteria and grown at 25°C. 5 days after seeding, animals that had only reached mid to late larval stages were considered developmentally arrested. (n=50; error bars based on S.D. from 3 independent experiments) (b-d) Eggs of *daf-2(e1370ts)* animals were seeded onto the indicated RNAi bacteria and grown at 25°C. (b) Loss of SWI/SNF impairs the longevity of these animals, as indicated by their reduced survival 9 days after seeding. Significant reductions are indicated (*; t-Test; p<0.05). (n=50; error bars based on S.D. from 3

independent experiments) (c,d) 5 days after seeding, *swsn-1* (RNAi) causes common absence of dauer-specific alae (c; yellow arrows) and occasional absence of the pharyngeal plug (d; red arrows indicate a closed, blue arrows an open pharynx) (scale bars: 10 μm). (e) Overexpression of SWSN-4/BRG1 or SWSN-1/BAF155/170 moderately promotes dauer formation in a *daf-16*-dependent manner. Eggs of wild-type, *daf-2(e1370ts)*, *daf-2(e1370ts); SWSN4::GFP OE* (GR1908), or *daf-2(e1370ts); SWSN1::GFP OE* (GR1900) animals were placed on either control or *daf-16* RNAi bacteria and grown at 22°C. Dauers were identified after 5 days based on morphology. Significant enhancements in dauer formation compared to *daf-2(e1370ts)* are indicated (*; t-Test; p<0.05). (n=50; error bars based on S.D. from 3 independent experiments).

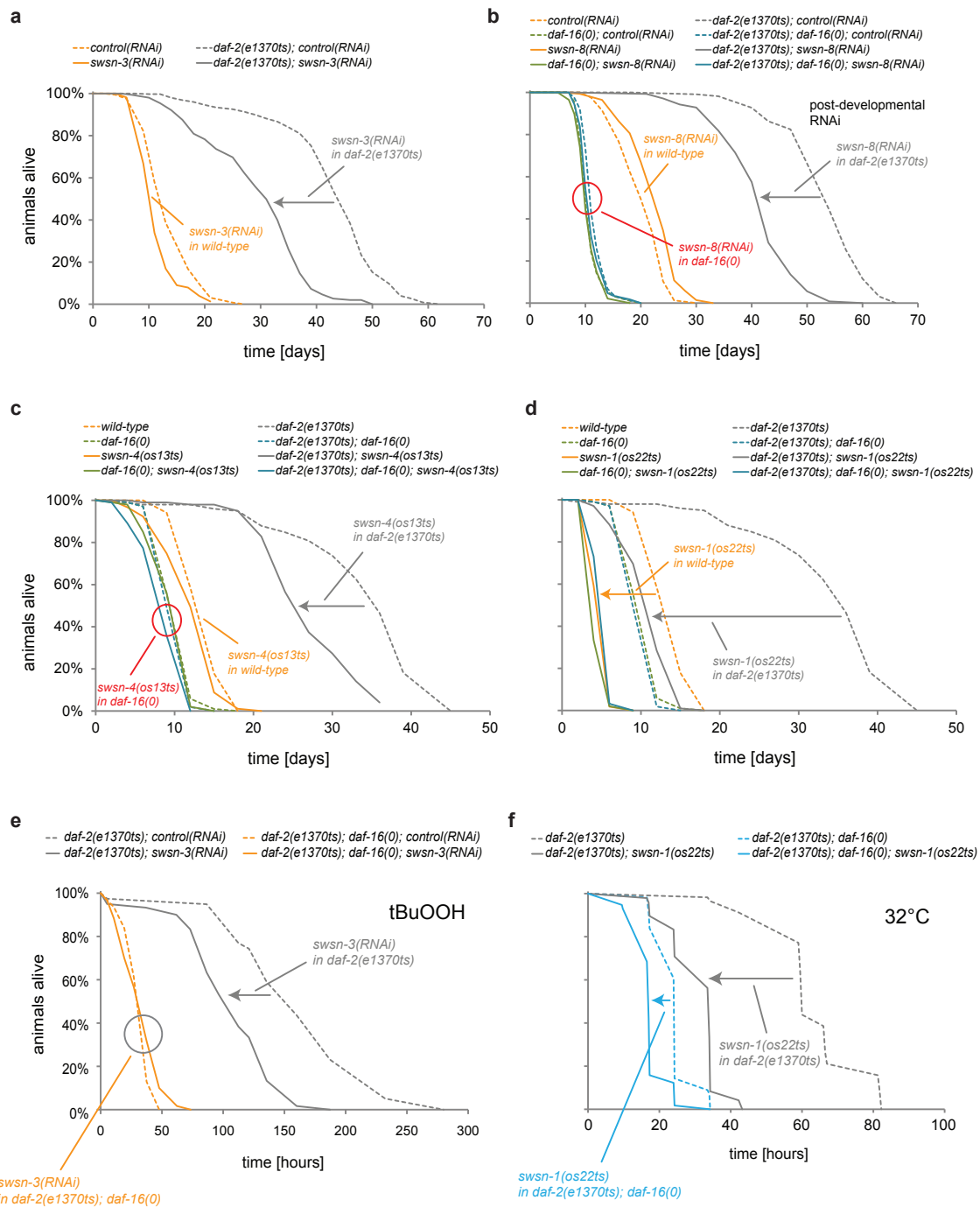


Figure S7 (a-d) Lifespan phenotypes caused by loss of SWI/SNF subunits. (a) Indicated *C. elegans* strains were grown from the L1-stage on the indicated RNAi bacteria. *e1370ts* was inactivated by a shift to restrictive temperature at the L4-stage. (b) Post-developmental RNAi. Indicated *C. elegans* strains were grown from the L1-stage on *E. coli* HT115. At the L4-stage, animals were shifted to the indicated RNAi bacteria and *e1370ts* was inactivated by shift to restrictive temperature. (c,d) Lifespan analyses of SWI/SNF mutant alleles. Indicated *C. elegans* strains were grown at permissive temperature until the L4-stage and then shifted to restrictive temperature, in order to inactivate the *e1370ts*, *os13ts*, and *os22ts* alleles. (e,f) Stress resistance phenotypes caused by loss of SWI/SNF subunits.

Animals were grown from the L1-stage on *E. coli* OP50 or the indicated RNAi bacteria. At the L4-stage, *e1370ts* and *os22ts* alleles were inactivated by shift to restrictive temperature. (e) Oxidative stress resistance assay. At day 1 of adulthood, animals were transferred to plates containing 6 mM t-Butylhydroperoxide (tBuOOH) and their survival was monitored. (f) Heat stress resistance assay. At day 1 of adulthood, animals were shifted to 32°C and their survival was monitored. All survival data (panels (a-f)) was obtained from a minimum of 100 animals per condition, mean survival times and S.E.M. were obtained by Kaplan-Meier analysis, and significant differences between conditions were determined by log-rank test (for exact numbers of animals and statistical data see Table S9).

Fig. 1a

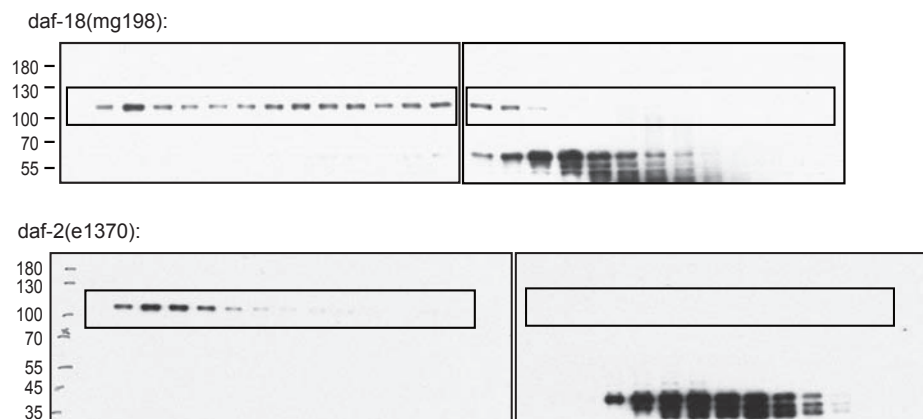


Fig. 1b

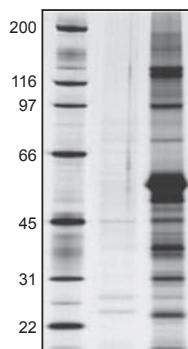


Fig. 1c

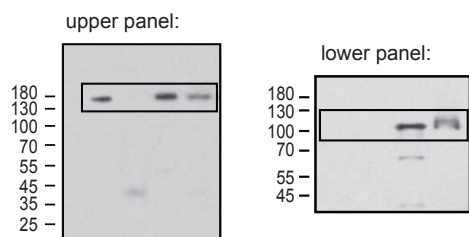


Fig. 1d

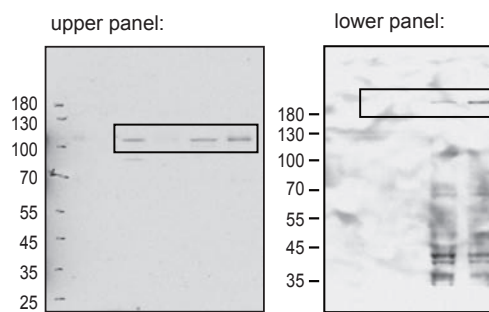


Figure S7 Uncropped key electrophoresis data.